Journal of Futures Markets

WILEY

RESEARCH ARTICLE

Pricing VIX Futures and Options With Good and Bad Volatility of Volatility

Zhiyu Guo[1,2] | Zhuo Huang[2,3] | Chen Tong[4,5]

[1]School of International Economics, China Foreign Affairs University, Beijing, China | [2]Institute of Digital Finance, Peking University, Beijing, China | [3]China Center for Economic Research, National School of Development, Peking University, Beijing, China | [4]Department of Finance, School of Economics & Wang Yanan Institute for Studies in Economics (WISE), Xiamen University, Xiamen, China | [5]Laboratory of Digital Finance, Xiamen University, Xiamen, China

Correspondence: Chen Tong (tongchen@xmu.edu.cn)

Received: 19 January 2024 | **Revised:** 3 April 2024 | **Accepted:** 13 July 2024

Funding: This research was supported by the Fund of the National Natural Science Foundation of China (72271010, 72241418), Youth Fund of the National Natural Science Foundation of China (72301227), and the Ministry of Education of China, Humanities and Social Sciences Youth Fund (22YJC790117).

Keywords: high-frequency VIX | realized semivariance | VIX futures and option pricing

ABSTRACT

This article studies the pricing of VIX futures and options by directly modeling the dynamics of VIX, based on realized semivariances computed from high-frequency data of VIX. We derive the closed-form pricing formula for both the VIX futures and options. The empirical results show that the new model provides superior pricing performance compared with the model based on conventional unsigned realized variance and the classic Heston-Nandi GARCH model, both in sample and out of sample. Our study confirms that the decomposition of realized variance into upside and downside components helps to improve the pricing performance for VIX futures and options.

JEL Classification: C51, C52, G12, G13

1 | Introduction

The CBOE VIX, as a measure of market implied volatility of S&P 500 index, has been widely studied over the past two decades. The launch of futures and options written on VIX in 2004 and 2006 enables investors to trade volatility directly and hedge their exposure of portfolio to volatility risk. Since then, VIX derivatives have become an important part of financial markets, which prompt researchers to devote more attention to study the valuation of VIX derivatives.

The literature on pricing VIX derivatives can be mainly divided into two categories. One strand is to model the dynamics of S&P 500 index (SPX) under the physical measure and then derive the pricing formulas for VIX and VIX derivatives after risk neutralization. Under the continuous-time framework, Zhang and Zhu (2006) explored the pricing of VIX futures by utilizing the Heston stochastic model of SPX. Sepp (2008) considered the VIX option pricing and assumed that the variance of SPX returns is driven by the Heston stochastic model with variance jumps. Other studies under the continuous-time framework include Lin (2007), Lin and Chang (2009), Lian and Zhu (2013), and Luo, Zhang, and Zhang (2019). Under the discrete-time framework, Wang et al. (2017) and Tong (2024) priced the CBOE VIX under affine and non-affine GARCH models, respectively.[1] Huang, Tong, and Wang (2019) and Wang and Wang (2020) adopted the HAR-gamma process with flexible leverage components (LHARG) and the GARV model with two hidden components and jump (GARV-2C-J) to depict the dynamics of SPX and price VIX futures, respectively. For VIX options, Cao et al. (2020) provided semi closed-form solutions under affine GARCH models, and Tong and Huang (2021) derived analytical pricing formulas when the SPX return follows the GARV and Realized GARCH models.

The second strand of the literature is to directly model the dynamics of VIX under the risk-neutral measure. For example, Grünbichler

and Longstaff (1996) used the mean-reverting square-root process to model the implied volatility index and price options, Goard and Mazur (2013) developed analytic solutions for VIX option prices when the VIX are modeled by the 3/2-model, and Mencia and Sentana (2013) compared the empirical performance of several models on pricing VIX derivatives. Other work under the continuous-time framework included Park (2016) and Jing, Li, and Ma (2020). For discrete-time models, the literature is more about pricing VIX futures: Yin, Bian, and Wang (2021) applied the HAR model with asymmetric jumps to model the logarithm of VIX and priced VIX futures. Based on a similar process, Tong, Huang, and Wang (2022) investigated the information role of VIX futures in pricing VIX options. Wang et al. (2022) extended the model in Yin, Bian, and Wang (2021) by incorporating dynamic volatility with short- and long-run components and dynamic jump intensity. The above-mentioned two studies only use daily series of VIX, not the information contained in the high-frequency data of VIX. Jiang et al. (2022) applied VIX 5-min high frequency data to identify the interday and intraday jumps of VIX and incorporated these jumps when modeling the logarithmic VIX to price VIX futures.

Modeling the dynamics of S&P 500 to price VIX derivatives can provide a consistent framework for the SPX, VIX, and VIX derivatives, but it can also induce inaccurate integration problems, and the computation is time consuming, while directly modeling the dynamics of VIX can overcome these problems. However, the majority of the literature on pricing VIX derivatives belongs to the first category, and the exploration of the second modeling method is still at the initial stage. Therefore, this paper studies VIX option pricing by directly modeling the dynamics of VIX.

It is well known that the realized variance computed from high-frequency data provides accurate measurement of latent volatility and thus improves the volatility forecasting and derivatives pricing. Further, Barndorff-Nielsen, Kinnebrock, and Shephard (2010) proposed to distinguish upside and downside components from realized variance, which are calculated by summing up intraday positive and negative returns, respectively. Existing studies showed that such decomposition of realized variance of SPX returns can improve volatility prediction (Patton and Sheppard 2015), VIX futures pricing (Tong and Huang 2023), and stock option pricing (Feunou and Okou 2019). However, the studies on the role of realized semivariance of VIX in derivatives pricing remain limited.

As a volatility index, the dynamics of VIX exhibit characteristics distinct from those of stock prices. The asymmetric leverage effect[2] dictates that volatility tends to escalate more significantly during stock price declines than it decreases during market upswings. This asymmetry implies that the realized upside volatility of VIX may manifest more pronounced peaks than its downside volatility. It also reveals the importance of separately modeling the upside and downside components. These insights, supported by the summary statistics presented in Table 1, underscore the potential impact of these unique characteristics on VIX options pricing. Therefore, this paper constructs the realized semivariance of VIX based on high-frequency VIX data and check if the distinction between realized upside and downside variances can improve the pricing performance for VIX futures and option. Considering the long-memory feature of volatility process, we take the heterogeneous autoregressive (HAR) framework and combine it with a realized semivariance-based model.

Our contributions are threefold. *First*, we contribute to the literature on pricing VIX futures and options by directly modeling VIX with realized semivariances. Our paper is closely related to Jiang et al. (2022) and Qiao and Jiang (2023), who priced VIX derivatives using high-frequency data of VIX. However, both of these two studies only focused on the pricing of VIX futures. The former investigated the impact of jumps on futures prices, and the latter combined realized the semivariance-based model with support vector regression (SVR) to price VIX futures. Our work is different from theirs since we provide a unified framework to jointly price VIX futures and options. And to the best of our knowledge (if any), this paper is the first to investigate the role of realized semivariance of VIX in pricing VIX options. *Second*, we drive the closed-form expressions of VIX futures price and option price under the proposed model, in which the moment generating function is expressed as a exponential linear function of contemporaneous and lagged logarithm VIX, as well as the conditional upside and downside variances. This makes the computation of futures and option prices much easier and time saving. *Third*, we conduct an extensive empirical analysis to investigate the pricing performance of the proposed realized semivariance-based model. We compare its in- and out-of-sample performance with the model based on conventional unsigned realized variance and the classic Heston-Nandi GARCH model. The empirical results show that the realized semivariance-based model performs best both in and out of sample, indicating that separating upside and downside realized variances of VIX is helpful to obtain more accurate prices of VIX futures and options.

The remainder of the paper is organized as follows: Section 2 introduces the realized semivariance-based model, HAR-RSV. Section 3 derives the pricing formulas of VIX futures and options under the HAR-RSV model. In Section 4, we introduce two competing models and derive their pricing formulas. Section 5 presents empirical analysis, where we describe the data, estimate the parameters, and investigate the pricing performance of the models, both in and out of sample. Finally, Section 6 concludes the paper.

2 | The Realized Semivariance-Based Model (HAR-RSV)

According to Barndorff-Nielsen, Kinnebrock, and Shephard (2010), for a given day t, the upside realized semivariance RV_t^u and the downside realized semivariance RV_t^d for the logarithm of the VIX_t, denoted as $y_t = \log \mathrm{VIX}_t$, are defined as

$$RV_t^u = \sum_{j=1}^{M_t} r_{t,j}^2 \mathbb{I}\{r_{t,j} > 0\},$$
$$RV_t^d = \sum_{j=1}^{M_t} r_{t,j}^2 \mathbb{I}\{r_{t,j} < 0\},$$

where $r_{t,j} = y_{t,j} - y_{t,j-1}$ is the jth intraday return during day t, M_t is the number of returns on that day, and $\mathbb{I}\{\cdot\}$ is the indicator function. By construction, the total realized variance, RV_t, is given by $RV_t = RV_t^u + RV_t^d$.

In this paper, we build a model to pricing VIX futures and options by incorporating the realized upside and downside variances of VIX into the conditional variance updating equations. Due to the long-memory feature of VIX, we consider an HAR structure for the dynamics of logarithm VIX. Under the risk-neutral measure, the dynamics of y_t are assumed to follow

$$\begin{aligned} y_{t+1} = w + \beta_d y_t^{(d)} + \beta_w y_t^{(w)} + \beta_m y_t^{(m)} + \left(\lambda_u - \frac{1}{2}\right)h_{u,t} \\ + \left(\lambda_d - \frac{1}{2}\right)h_{d,t} + \sqrt{h_{u,t}}\epsilon_{u,t+1}^{(1)} + \sqrt{h_{d,t}}\epsilon_{d,t+1}^{(1)}, \end{aligned} \tag{1}$$

where $y_t^{(d)}, y_t^{(w)}$, and $y_t^{(m)}$ are, respectively, the daily, weekly, and monthly components in the HAR framework:

$$\begin{cases} y_t^{(d)} = y_t, \\ y_t^{(w)} = \dfrac{1}{4}\displaystyle\sum_{i=2}^{5} y_{t+1-i}, \\ y_t^{(m)} = \dfrac{1}{17}\displaystyle\sum_{i=6}^{22} y_{t+1-i}. \end{cases} \tag{2}$$

The conditional variance of y_{t+1} is h_t, which is the sum of conditional upside variance $h_{u,t}$ and downside variance $h_{d,t}$, where $h_{u,t}$ and $h_{d,t}$ correspond to the expected realized semivariances. The innovations consist of two independent Gaussian shocks $\epsilon_{i,t+1}^{(1)} \sim N(0,1)$ for $i = u, d$. The terms $(\lambda_u - \frac{1}{2})h_{u,t}$ and $(\lambda_d - \frac{1}{2})h_{d,t}$ can be interpreted as compensations for upside and downside volatility risk of VIX.

We assume that the information about realized upside and downside variances at day t is used to update the conditional semivariances of y_{t+1}:

$$h_{u,t} = w_u + b_u h_{u,t-1} + a_u RV_t^u, \tag{3}$$

$$h_{d,t} = w_d + b_d h_{d,t-1} + a_d RV_t^d, \tag{4}$$

where $w_i > 0, b_i > 0$ and $a_i > 0$, for $i = u, d$. By introducing measurement errors $\epsilon_{i,t}^{(2)} \sim N(0,1)$ for $i = u, d$, the measurement equations are specified as follows:

$$RV_{t+1}^u = h_{u,t} + \sigma_u\left[\left(\epsilon_{u,t+1}^{(2)} - \gamma_u\sqrt{h_{u,t}}\right)^2 - \left(1 + \gamma_u^2 h_{u,t}\right)\right], \tag{5}$$

$$RV_{t+1}^d = h_{d,t} + \sigma_d\left[\left(\epsilon_{d,t+1}^{(2)} - \gamma_d\sqrt{h_{d,t}}\right)^2 - \left(1 + \gamma_d^2 h_{d,t}\right)\right], \tag{6}$$

where $\epsilon_{i,t}^{(2)}$ has correlation ρ_i with $\epsilon_{i,t}^{(1)}$. This setting is consistent with the measurement equation in the GARV model proposed by Christoffersen et al. (2014). The above equations can result in $E_t[RV_{t+1}^u] = h_{u,t}$, $E_t[RV_{t+1}^d] = h_{d,t}$, thus $E_t[RV_{t+1}] = h_t$. To make the variance processes stationary, the parameters further satisfy the constraint conditions $b_i + a_i < 1$. We call the model described in this subsection as the HAR-RSV model.

3 | The Pricing Formulas of VIX Futures and Options

We first derive the pricing formulas of VIX futures and options under the HAR-RSV model. Let $f_{t,T}(\phi)$ be the conditional moment generating function (MGF) of y_T, that is,

$$f_{t,T}(\phi) = E_t[\exp(\phi y_T)]. \tag{7}$$

And an analytical form of $f_{t,T}(\phi)$ is crucial for deriving closed-from pricing formula for VIX futures and options. The form of $f_{t,T}(\phi)$ is given by the following Proposition 1.

Proposition 1. *Suppose that $y_t = \log \mathrm{VIX}_t$ follows the HAR-RSV process, then the conditional moment generating function of y_T takes the following log-linear form:*

$$\begin{aligned} f_{t,T}(\phi) = \exp\Bigg(A(m,\phi) + \sum_{i=1}^{22} B_i(m,\phi)y_{t+1-i} + C(m,\phi)h_{u,t} \\ + D(m,\phi)h_{d,t}\Bigg), \end{aligned} \tag{8}$$

where $m = T - t$, and $A(m,\phi), B_i(m,\phi), C(m,\phi), D(m,\phi)$ are given by:

$$\begin{aligned} A(m+1,\phi) &= A(m,\phi) + B_1(m,\phi)w + C(m,\phi)w_u - C(m,\phi)a_u\sigma_u + D(m,\phi)w_d - D(m,\phi)a_d\sigma_d \\ &\quad - \frac{1}{2}\ln(1 - 2C(m,\phi)a_u\sigma_u) - \frac{1}{2}\ln(1 - 2D(m,\phi)a_d\sigma_d), \\ C(m+1,\phi) &= B_1(m,\phi)\left(\lambda_u - \frac{1}{2}\right) + C(m,\phi)b_u + C(m,\phi)a_u + \frac{B_1^2(m,\phi)}{2 - 4C(m,\phi)a_u\sigma_u} \\ &\quad + \frac{C(m,\phi)a_u\sigma_u\left(2\gamma_u^2 C(m,\phi)a_u\sigma_u - 2\gamma_u B_1(m,\phi)\rho_u - B_1^2(m,\phi)\left(1 - \rho_u^2\right)\right)}{1 - 2C(m,\phi)a_u\sigma_u}, \\ D(m+1,\phi) &= B_1(m,\phi)\left(\lambda_d - \frac{1}{2}\right) + D(m,\phi)b_d + D(m,\phi)a_d + \frac{B_1^2(m,\phi)}{2 - 4D(m,\phi)a_d\sigma_d} \\ &\quad + \frac{D(m,\phi)a_d\sigma_d\left(2\gamma_d^2 D(m,\phi)a_d\sigma_d - 2\gamma_d B_1(m,\phi)\rho_d - B_1^2(m,\phi)\left(1 - \rho_d^2\right)\right)}{1 - 2D(m,\phi)a_d\sigma_d}, \end{aligned}$$

with

$$B_i(m+1,\phi)=\begin{cases}B_1(m,\phi)\beta_d+B_2(m,\phi) & i=1,\\ \frac{1}{4}B_1(m,\phi)\beta_w+B_{i+1}(m,\phi) & 2\le i\le 5,\\ \frac{1}{17}B_1(m,\phi)\beta_m+B_{i+1}(m,\phi) & 6\le i\le 21,\\ \frac{1}{17}B_1(m,\phi)\beta_m & i=22.\end{cases}$$

The terminal conditions are $B_1(0,\phi)=\phi, B_i(0,\phi)=0$ *for* $i\ge 2, A(0,\phi)=C(0,\phi)=D(0,\phi)=0$.

Proof. See Appendix A. □

Since we directly model the dynamics of VIX under the risk-neutral measure, the price of VIX futures at time t with a maturity date T is given by the expectation

$$F_{t,T}=E_t^Q[\mathrm{VIX}_T]=E_t[\exp(y_T)], \tag{9}$$

which is the value of the conditional moment generating function $f_{t,T}(\phi)$ at $\phi=1$.

As for the VIX call option price, it can be written as follows:

$$\begin{aligned}C_t&=e^{-r(T-t)}E_t^Q[\max(\mathrm{VIX}_T-K,0)]\\&=e^{-r(T-t)}E_t^Q[\max(\exp(y_T)-K,0)]\\&=e^{-r(T-t)}\left[\int_{\ln K}^{\infty}\exp(x)p(x)dx-K\int_{\ln K}^{\infty}p(x)dx\right],\end{aligned}$$

where $p(\cdot)$ is the conditional probability density function of y_T. By using a same mathematical technique in Heston and Nandi (2000), C_t can be further expressed in the following proposition 2, which can be evaluated by using the analytical expression of $f_{t,T}(\phi)$ provided in Proposition 1.

Proposition 2. *If the conditional characteristic function of* $y_T=\log \mathrm{VIX}_T$ *is* $f_{t,T}(i\phi)$, *then the price of a European VIX call option at time* t *with strike price* K *and maturity date* T *is expressed by*

$$C_t=e^{-r(T-t)}[f_{t,T}(1)P_{1,t}-KP_{2,t}],$$

with

$$\begin{aligned}P_{1,t}&=\frac{1}{2}+\frac{1}{\pi}\int_0^{\infty}\mathrm{Re}\left[\frac{K^{-i\phi}f_{t,T}(i\phi+1)}{i\phi f_{t,T}(1)}d\phi\right],\\P_{2,t}&=\frac{1}{2}+\frac{1}{\pi}\int_0^{\infty}\mathrm{Re}\left[\frac{K^{-i\phi}f_{t,T}(i\phi)}{i\phi}d\phi\right],\end{aligned}$$

where $i=\sqrt{-1}$ and $\mathrm{Re}[x]$ takes the real part of x.

4 | Competing Models

We consider two competing models and compare their pricing performances with our proposed HAR-RSV model. The first competing model incorporates realized variance but does not distinguish the upside and downside realized semivariance; we call it the HAR-RV model. The second competing model uses the Heston-Nandi GARCH model for the conditional variance equation, and we call it the HAR-Heston-Nandi GARCH model (abbreviated as HAR-HNG hereafter).

4.1 | HAR-RV Model

The dynamics of logarithm VIX, y_t, are given by

$$\begin{aligned}y_{t+1}=w+\beta_d y_t^{(d)}+\beta_w y_t^{(w)}+\beta_m y_t^{(m)}+\left(\lambda-\frac{1}{2}\right)h_t\\+\sqrt{h_t}\epsilon_{t+1}^{(1)},\end{aligned} \tag{10}$$

where $y_t^{(d)}, y_t^{(w)}$, and $y_t^{(m)}$ are given by Equation (2). Here the innovation only consists of one single Gaussian shock $\epsilon_{t+1}^{(1)}\sim N(0,1)$. The conditional variance h_{t+1} is updated according to the realized variance,

$$h_t=w_h+bh_{t-1}+aRV_t. \tag{11}$$

The realized variance RV_{t+1} is linked with its expectation h_t according to the following measurement equation:

$$RV_{t+1}=h_t+\sigma\left[\left(\epsilon_{t+1}^{(2)}-\gamma\sqrt{h_t}\right)^2-\left(1+\gamma^2h_t\right)\right], \tag{12}$$

where $\epsilon_t^{(2)}\sim N(0,1)$ has correlation ρ with $\epsilon_t^{(1)}$. The above equation implies $E_t[RV_{t+1}]=h_t$. Under the HAR-RV model, the moment generating function of y_T is given by

$$f_{t,T}(\phi)=\exp\left(A(m,\phi)+\sum_{i=1}^{22}B_i(m,\phi)y_{t+1-i}+C(m,\phi)h_t\right), \tag{13}$$

where $m=T-t$ and $A(m,\phi), B_i(m,\phi), C(m,\phi)$ are given by

$$\begin{aligned}A(m+1,\phi)=A(m,\phi)+B_1(m,\phi)w+C(m,\phi)(w_h-a\sigma)\\-\frac{1}{2}\ln(1-2C(m,\phi)a\sigma),\end{aligned} \tag{14}$$

$$\begin{aligned}C(m+1,\phi)=B_1(m,\phi)\left(\lambda-\frac{1}{2}\right)+C(m,\phi)(b+a)+\frac{B_1^2(m,\phi)}{2-4C(m,\phi)a\sigma}\\+\frac{C(m,\phi)a\sigma\left(2\gamma^2C(m,\phi)a\sigma-2\gamma B_1(m,\phi)\rho-B_1^2(m,\phi)(1-\rho^2)\right)}{1-2C(m,\phi)a\sigma},\end{aligned} \tag{15}$$

with

$$B_i(m+1,\phi)=\begin{cases}B_1(m,\phi)\beta_d+B_2(m,\phi) & i=1,\\ \frac{1}{4}B_1(m,\phi)\beta_w+B_{i+1}(m,\phi) & 2\le i\le 5,\\ \frac{1}{17}B_1(m,\phi)\beta_m+B_{i+1}(m,\phi) & 6\le i\le 21,\\ \frac{1}{17}B_1(m,\phi)\beta_m & i=22.\end{cases}$$

The terminal condition is $B_1(0,\phi)=\phi, B_i(0,\phi)=0$ for $i\ge 2, A(0,\phi)=C(0,\phi)=0$. Proof is given in Appendix B. After getting the moment generating function $f_{t,T}(\phi)$ under HAR-RV model, the futures price is the value of $f_{t,T}(\phi)$ at $\phi=1$, and option price can be obtained by using the formula given in Proposition 2.

4.2 | HAR-HNG Model

Under the HAR-HNG model, the dynamics of logarithm VIX, y_t, are described by

$$y_{t+1}=w+\beta_d y_t^{(d)}+\beta_w y_t^{(w)}+\beta_m y_t^{(m)}+\left(\lambda-\frac{1}{2}\right)h_t+\sqrt{h_t}\epsilon_{t+1}, \tag{16}$$

The conditional variance updating equation is given as follows:

$$h_{t+1}=w_h+bh_t+a(\epsilon_{t+1}-\gamma\sqrt{h_t})^2. \tag{17}$$

This model does not incorporate any realized measures in the variance updating equation, and only daily series of VIX are needed. Under the HAR-HNG model, the moment generating function of y_T is given by

$$f_{t,T}(\phi)=\exp\left(A(m,\phi)+\sum_{i=1}^{22}B_i(m,\phi)y_{t+1-i}+C(m,\phi)h_t\right), \tag{18}$$

where $B_i(m,\phi)$ can be obtained in a similar way of HAR-RV; see Appendix C for more details. After getting the moment generating function $f_{t,T}(\phi)$ under the HAR-HNG model, the prices of VIX futures and options can be obtained.

5 | Empirical Analysis

5.1 | Data

To construct the realized upside and downside variances of VIX, we collect the intraday high-frequency VIX data from TickData.com. The realized semivariances are computed using the 5-min VIX log-returns to avoid the microstructure problem. Figure 1 plots the time series of the daily VIX and logarithmic VIX, along with the realized volatility and its upside component (square root of realized variance and upside realized variance), and the difference between upside and downside realized volatilities.

The highest level of volatility occurred on August 24, 2015, marking the beginning of a stock market crash. On that day, the VIX level rose to 50.78 from 28.03, then dropped to 40.62 at closing. The realized volatility on August 24, 2015 was 0.6340, with the upside component at 0.5964, accounting for 94.07% of the total realized volatility. This corresponds to the highest point of the bottom right subfigure of Figure 1. For the second highest realized volatility, the downside component has more weight, although the difference between the upside and downside components is not so big. Overall, when the realized volatility of VIX is extremely high, the upside component tends to account for a more substantial portion.

Table 1 further presents the summary statistics of annualized realized volatility, upside and downside volatility, and VIX itself. We can see that RV^u and RV^d have similar magnitudes, as their means and medians are very close. This is because the difference between upside and downside realized volatilities is overall symmetric, as shown in the bottom right subfigure of Figure 1. While there are outliers with exceptionally high values in the realized upside volatilities, their influence on the overall mean and median is constrained when analyzing a substantial number of observations. However, RV^u exhibits a larger standard deviation, skewness, and kurtosis[3], particularly in terms of kurtosis, which is more than two times higher than that of RV^d.

To evaluate the empirical performance of the proposed HAR-RSV model on pricing VIX futures and options, we collect a panel of VIX futures prices and option prices from CBOE's website. The full sample of futures contracts spans a 17-year period from March 31, 2004 to October 27, 2020, while the full sample of VIX option contracts spans a 15-year period from March 1, 2006 to October 15, 2020. Tables 2 and 3 present the summary statistics of the VIX futures and options contracts in our sample, respectively. Note that as VIX calls have much higher trading volumes than the puts, we consider only VIX call options following Song and Xiu (2016), Tong and Huang (2021), and Luo, Zhang, and Zhang (2019).

Table 2 shows that our sample consists of 29,807 futures contracts, with an average VIX futures value of 20.85. We further categorize the contracts based on the VIX level and days to maturity. The majority of futures contracts are associated with a VIX level smaller than 20, in which VIX futures with VIX level below 15 account for 42.3% of the total contracts, while those with a VIX level between 15 and 20 account for 28.15%. The average futures prices increase with the VIX level, confirming a close relationship between VIX futures prices and the spot VIX level. The standard deviation generally increases as the VIX level increases and as the days to maturity decrease.

To assess the performance of option pricing, we conduct in-sample analysis using Wednesday contracts and out-of-sample analysis using Thursday contracts. Table 3 presents the summary statistics of the VIX call option contracts for both on Wednesday and Thursday.

Table 3 shows there are 45,945 Wednesday call option contracts and 45,446 Thursday contracts in our sample, with average VIX option prices of 1.653 and 1.639, respectively. We further divide

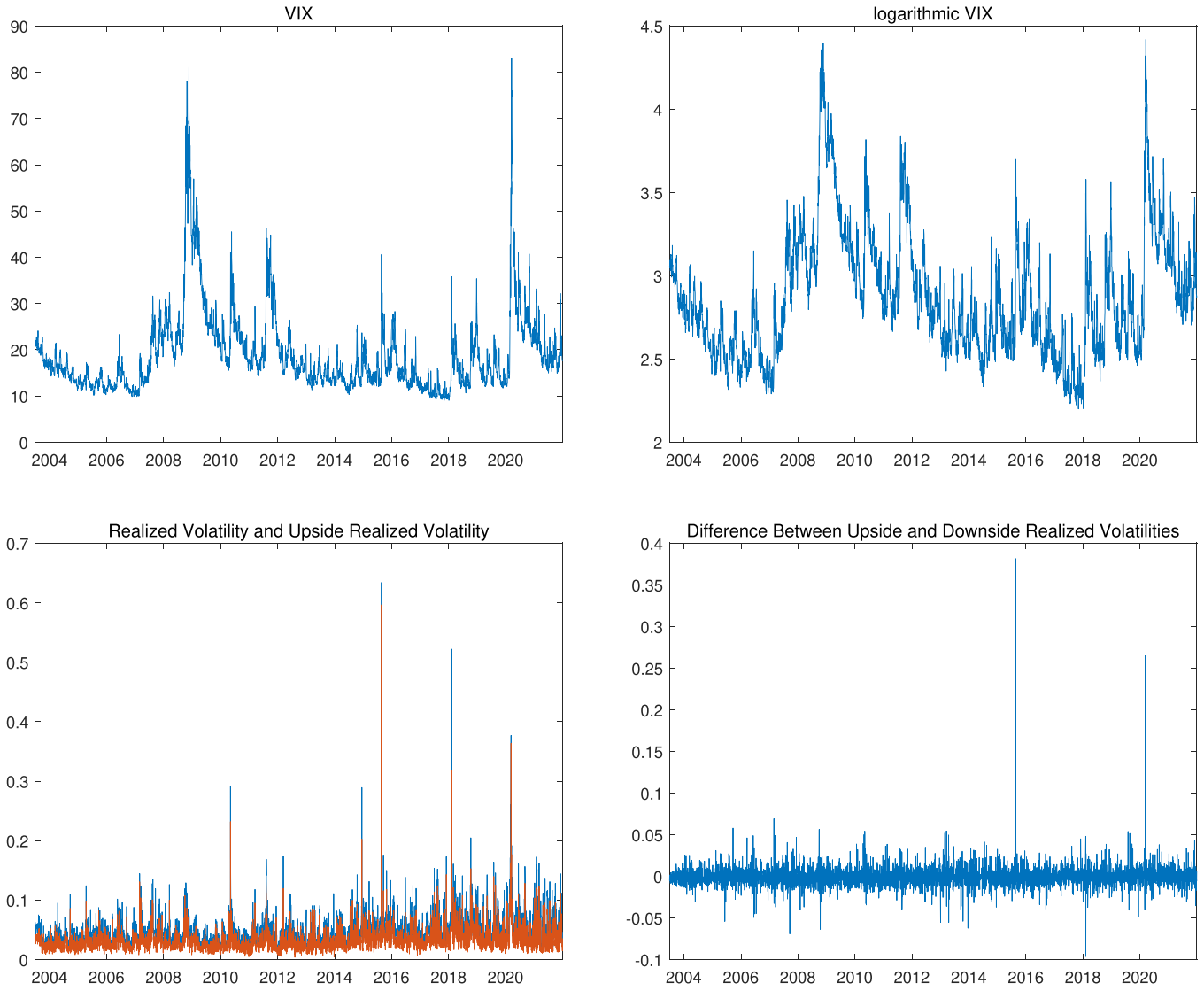

FIGURE 1 | Daily time series of CBOE VIX and its realized volatilities.

TABLE 1 | Summary statistics of historical series.

	Mean	Median	Std. dev.	Skewness	Kurtosis	Max	Min
Realized volatility	75.92	65.99	43.71	5.32	77.00	1006.43	15.61
Upside volatility	52.97	45.33	34.61	6.54	121.51	946.75	5.99
Downside volatility	53.10	46.49	29.18	4.11	52.61	657.27	7.31
VIX	18.94	16.40	8.88	2.65	12.83	83.05	9.03

Note: Summary statistics for the realized volatility of VIX, upside and downside volatility of VIX, and VIX level, where realized volatility and upside and downside volatility are annualized by the transformation $100\sqrt{252 \times RV}$, etc.

the contracts according to the moneyness and days to maturity. The majority of option contracts are out of the money ($m < 0$), accounting for approximately 76% of total contracts. The distribution of contracts across different days to maturity is relatively uniform. Additionally, the average option prices increase with the moneyness and maturity, and the average implied volatilities decrease with the moneyness and maturity.

5.2 | Parameter Estimation

5.2.1 | Parameter Estimation Using Futures Contracts

In the analysis of futures pricing, we estimate the parameters of the proposed HAR-RSV model and the two competing models by maximizing the likelihood of pricing errors. Given a set of

TABLE 2 | Summary statistics of VIX futures contracts.

	Obs.	Mean	STD	Skew	Kurt	Min	Max
All	29,807	20.85	6.54	1.66	7.05	9.91	71.15
Partitioned by VIX level							
VIX < 15	12,607	16.29	2.23	0.49	4.63	9.91	27.60
15 ≤ VIX < 20	8391	20.12	3.11	0.74	3.03	13.50	31.00
20 ≤ VIX < 25	4120	24.21	3.53	0.31	2.26	16.70	33.30
25 ≤ VIX < 30	2079	27.22	3.70	−0.42	2.41	17.69	35.39
30 ≤ VIX < 35	958	30.41	3.59	−1.26	4.19	17.65	38.40
35 ≤ VIX	1652	37.41	7.82	0.47	3.85	18.73	71.15
Partitioned by days to maturity							
DTM < 30	3738	19.51	8.42	2.23	9.26	9.91	71.15
30 ≤ DTM < 90	7495	20.65	7.32	1.67	6.38	11.45	60.10
90 ≤ DTM < 150	7243	21.42	6.42	1.31	4.63	12.54	52.38
150 ≤ DTM < 210	6726	21.64	5.69	1.16	3.91	13.53	45.99
210 ≤ DTM	4605	20.21	4.08	1.36	4.58	14.30	37.35

Note: This table presents the summary statistics of VIX futures contracts from March 31, 2004 to October 27, 2020. DTM denotes the days to maturity.

TABLE 3 | Summary statistics of VIX option contracts.

	Wednesday			Thursday		
	Obs.	Avg. price	Avg. impv	Obs.	Avg. price	Avg. impv
All	45,945	1.653	0.996	45,446	1.639	1.004
Partitioned by moneyness, $m = \log(F/K)$						
$m < -0.4$	16,777	0.470	1.207	16,579	0.484	1.221
$-0.4 \le m < -0.2$	9597	1.062	1.015	9645	1.063	1.027
$-0.2 \le m < -0.1$	4499	1.591	0.920	4403	1.601	0.924
$-0.1 \le m < 0$	4085	2.085	0.849	4131	2.113	0.857
$0 \le m < 0.1$	3811	2.754	0.793	3698	2.742	0.794
$0.1 \le m$	7176	4.416	0.713	6990	4.335	0.708
Partitioned by days to maturity						
DTM < 20	7179	1.030	1.296	6843	1.028	1.328
20 ≤ DTM < 40	7009	1.320	1.143	10,215	1.356	1.120
40 ≤ DTM < 60	8630	1.655	1.002	5688	1.715	0.988
60 ≤ DTM < 80	7876	1.796	0.923	7875	1.793	0.925
80 ≤ DTM < 100	7181	1.964	0.855	6950	1.939	0.858
100 ≤ DTM	8070	2.078	0.791	7875	2.066	0.793

Note: This table presents the characteristics of VIX call option data by moneyness and maturity. The sample period starts on March 1, 2006, and ends on October 15, 2020. The moneyness is measured by $m = \log(F/K)$, where F is the futures price of VIX and K is the strike price. DTM denotes days to maturity.

parameters, the pricing error of each futures contract j is computed as follows:

$$e_j = F_j^{Mkt} - F_j^{Mod}, \tag{19}$$

where F_j^{Mkt} represents the market futures price, and F_j^{Mod} represents the model-based futures price. We assume that the pricing errors follow a normal distribution with a zero mean and a variance s^2 with the following log-likelihood function

$$\ln L = -\frac{1}{2}\sum_{j=1}^{N}\left(\ln(2\pi s^2) + \frac{e_j^2}{s^2}\right), \tag{20}$$

where N is the number of futures contracts in the sample. We can get the parameter estimations by maximizing

TABLE 4 | Parameter estimation using VIX futures contracts.

	HAR-RSV	HAR-RV	HAR-HNG
w	0.0297	0.0216	0.0229
β_d	0.8651	0.8947	0.9081
β_w	0.0498	9.09E−06	2.94E−09
β_m	0.0794	0.0971	0.0857
$\lambda_u(\lambda)$	−0.6720	0.3118	−1.5622
λ_d	−3.1683		
$w_u(w_h)$	7.62E−07	6.29E−04	5.18E−05
w_d	2.98E−05		
$b_u(b)$	0.9989	0.9862	0.9524
b_d	0.9514		
$a_u(a)$	9.57E−04	1.39E−04	3.18E−08
a_d	0.0378		
$\sigma_u(\sigma)$	0.0027	1.7518	
σ_d	3.57E−04		
$\gamma_u(\gamma)$	−222.2185	115.1940	413.8801
γ_d	−40.8975		
$\rho_u(\rho)$	−0.9572	−0.9997	
ρ_d	−0.9998		

Note: This table reports the estimation results for the three models using futures contracts for the period starting on March 31, 2004, and ending on October 27, 2020. The parameter notation in the bracket is for the HAR-RV and HAR-HNG models.
Abbreviations: HAR, heterogeneous autoregressive; HNG, Heston-Nandi GARCH; RSV, realized semivariance; RV, realized variance.

TABLE 5 | Parameter estimation using VIX option contracts.

	HAR-RSV	HAR-RV	HAR-HNG
w	0.0369	0.0256	0.0185
β_d	0.8679	0.9301	0.9133
β_w	0.0591	0.0117	0.0169
β_m	0.0687	0.0518	0.0638
$\lambda_u(\lambda)$	−1.1301	−0.2195	0.0812
λ_d	−3.2827		
$w_u(w_h)$	1.07E−05	9.79E−04	8.33E−04
w_d	1.06E−05		
$b_u(b)$	0.9990	0.9118	0.7733
b_d	0.9443		
$a_u(a)$	5.66E−04	2.50E−03	2.93E−06
a_d	0.0511		
$\sigma_u(\sigma)$	2.13E−03	0.0505	
σ_d	5.70E−04		
$\gamma_u(\gamma)$	980.4967	123.3745	−266.0089
γ_d	128.9998		
$\rho_u(\rho)$	−0.9378	−0.9851	
ρ_d	−0.9994		

Note: This table reports the estimation results for the three models using Wednesday call contracts for the period starting on March 1, 2006, and ending on October 15, 2020. The parameter notation in the bracket is for the HAR-RV and HAR-HNG models.
Abbreviations: HAR, heterogeneous autoregressive; HNG, Heston-Nandi GARCH; RSV, realized semivariance; RV, realized variance.

the above pricing error likelihood. This estimation method is equivalent to minimizing the sum of squared errors $\sum_{j=1}^{N} e_j^2$.

Table 4 reports the estimation results for the three models considered. From Table 4, we can see that for all models, the estimates of β_d and β_m significantly differ from zero, while the magnitudes of estimates of β_w are relatively smaller.[4] This suggests that the daily lag has the most substantial impact on explaining the current VIX level, followed by the monthly component, with the weekly component having the least influence. The sum of β_d, β_w, and β_m is very close to one, indicating a high level of persistence in the log VIX series. In the HAR-RSV model, both the estimates of λ_u and λ_d are negative, but the values are significantly different, signifying distinct impacts of upside and downside variances on log VIX. The leverage effect related parameters, γ_u and γ_d, also differ significantly, with the absolute value of γ_u being much larger than that of γ_d, indicating a more pronounced leverage effect for upside variance.

5.2.2 | Parameter Estimation Using Option Contracts

For option pricing analysis, we estimate the parameters of the HAR-RSV, HAR-RV, and HAR-HNG models by matching the model-implied VIX option prices with the option prices from the market that minimizes the root of mean squared pricing errors (RMSE).

Table 5 reports the parameter estimation results of the three models we consider based on Wednesday option contracts. These estimates show similar patterns to the results estimated using futures contracts, which confirms the different impact of upside and downside variances on log VIX.

5.3 | VIX Futures and Options Pricing Performance

We employ three error measures to evaluate the pricing performance of the three models, the root mean square error, mean absolute error, and mean absolute percentage error, which are defined as the following three equations,

$$\text{RMSE} = \sqrt{\frac{1}{N}\sum_{j=1}^{N}\left(c_j^{Mkt} - c_j^{Mod}\right)^2}, \tag{21}$$

$$\text{MAE} = \frac{1}{N}\sum_{j=1}^{N}\left|c_j^{Mkt} - c_j^{Mod}\right|, \tag{22}$$

$$\text{MAPE} = \frac{1}{N}\sum_{j=1}^{N}\left|1 - c_j^{Mod}/c_j^{Mkt}\right|, \tag{23}$$

where c_j^{Mkt} is the market option or futures price, c_j^{Mod} is the model-implied option or futures price, and N is the total number of available derivatives prices.

5.3.1 | VIX Futures Pricing Performance

Table 6 shows the in-sample pricing performances of the three models. We report the values of RMSE, MAE, and MAPE for the HAR-HNG model. For the HAR-RSV and HAR-RV models, we report the ratios of their RMSEs, MAEs, and MAPEs to the HNG model. Therefore, a ratio smaller than 1 indicates a better performance than HAR-HNG model and vice versa. We report the full-sample errors in the first row, and the pricing errors for contracts sorted by VIX level and days to maturity below.

Table 6 shows that the HAR-RSV model consistently outperforms the other models in all subgroups. When examining the six subgroups categorized by the VIX level, the outperformance of the HAR-RSV model is most evident when the VIX level ranges between 20 and 25, while its advantage is least pronounced for VIX levels between 30 and 35. Interestingly, when the VIX level exceeds 35, the HAR-HNG model performs better than the HAR-RV model. Across the five subgroups categorized by days to maturity, the outperformance of the HAR-RSV model becomes more noticeable as the days to maturity increases.

To check if there exists in-sample overfitting, we further conduct an out-of-sample analysis to evaluate the VIX futures pricing performance of the HAR-RSV model. We use the prices of VIX futures contracts from March 31, 2004 to December 31, 2019 to estimate the parameters and then use VIX futures contracts in 2020 to calculate the pricing errors. Such out-of-sample evaluation method is widely used in studies on derivatives pricing, see for example, Christoffersen and Jacobs (2004), and Tong, Hansen, and Huang (2022).

Table 7 presents the out-of-sample results, and it shows that the HAR-RSV model continues to outperform the competing models overall, with its superiority being even more evident in the out-of-sample case. However, it is worth noting that in certain subsamples, the HAR-RSV model may underperform the other models. Specifically, when the VIX level is below 20, the HAR-RSV model performs worse than the HAR-HNG model but better than the HAR-RV model. In the VIX range of 20–25, the HAR-RV model is the top performer, followed by the HAR-HNG model, and then the HAR-RSV model. However, when the VIX level exceeds 25, the HAR-RSV model outperforms the HAR-HNG model significantly, with pricing errors approximately half those of the HAR-HNG model. Overall, the HAR-RSV model performs better when the VIX level is high. When partitioning the samples by days to maturity, the HAR-RSV model consistently performs best, and the HAR-HNG model consistently exhibits the largest pricing errors.

5.3.2 | VIX Option Pricing Performance

Table 8 reports the in-sample pricing performance of the three aforementioned models for VIX options. Similarly, we report the values of RMSE, MAE, and MAPE for the HAR-HNG model and the ratios to the HNG model for the HAR-RSV and HAR-RV models. We report the full-sample errors in the first row and the pricing errors for contracts sorted by moneyness and days to maturity below.

Table 8 shows that the HAR-RSV model generally performs best in terms of RMSE, MAE and MAPE. Compared to the HAR-HNG model, the HAR-RSV and HAR-RV models show potential for up to a 30% reduction in pricing errors, highlighting the value of incorporating realized volatility of VIX in improving VIX option pricing accuracy.

TABLE 6 | In-sample VIX futures pricing performance.

	RMSE	Ratio to HNG		MAE	Ratio to HNG		MAPE	Ratio to HNG	
	HNG	RSV	RV	HNG	RSV	RV	HNG	RSV	RV
Full sample	**2.396**	0.780	0.996	**1.745**	0.755	0.981	**0.080**	0.768	0.980
Partitioned by VIX level									
VIX < 15	**1.417**	0.829	0.939	**1.025**	0.872	0.957	**0.062**	0.866	0.966
15 ≤ VIX < 20	**2.500**	0.764	0.982	**1.946**	0.744	0.979	**0.093**	0.755	0.983
20 ≤ VIX < 25	**3.025**	0.666	0.982	**2.465**	0.616	0.966	**0.099**	0.610	0.966
25 ≤ VIX < 30	**2.968**	0.791	0.954	**2.436**	0.724	0.933	**0.090**	0.727	0.935
30 ≤ VIX < 35	**2.609**	0.954	1.002	**2.094**	0.907	1.022	**0.071**	0.916	1.022
35 ≤ VIX	**4.321**	0.847	1.101	**3.359**	0.742	1.100	**0.096**	0.739	1.101
Partitioned by days to maturity									
DTM < 30	**1.535**	0.890	0.996	**0.941**	0.860	1.012	**0.045**	0.867	1.020
30 ≤ DTM < 90	**2.143**	0.838	0.990	**1.525**	0.781	0.940	**0.068**	0.806	0.943
90 ≤ DTM < 150	**2.449**	0.784	1.025	**1.817**	0.776	1.034	**0.080**	0.813	1.064
150 ≤ DTM < 210	**2.623**	0.773	1.048	**1.984**	0.760	1.075	**0.089**	0.777	1.088
210 ≤ DTM	**2.881**	0.700	0.900	**2.296**	0.659	0.831	**0.115**	0.641	0.788

Note: This table reports the in-sample VIX futures pricing performance of the three models described in Section 2. We suppress the notations "HAR" for convenience. We use contracts for the period starting on March 31, 2004, and ending on October 27, 2020. The pricing performance is evaluated through the root-mean squared error (RMSE), the mean absolute error (MAE), and the mean absolute percentage error (MAPE). The RMSEs, MAEs, and MAPEs of the benchmark HNG model are in bold font. For the RSV and RV models, we report the ratios of their RMSEs, MAEs, and MAPEs to the HNG model. We report the pricing errors for contracts sorted by VIX level and days to maturity.

TABLE 7 | Out-of-sample VIX futures pricing performance.

	RMSE	Ratio to HNG		MAE	Ratio to HNG		MAPE	Ratio to HNG	
	HNG	RSV	RV	HNG	RSV	RV	HNG	RSV	RV
Full sample	**6.232**	0.537	0.759	**4.675**	0.499	0.674	**0.154**	0.513	0.692
Partitioned by VIX level									
VIX < 15	**0.900**	1.178	1.311	**0.775**	1.151	1.241	**0.046**	1.136	1.241
15 ≤ VIX < 20	**1.077**	1.183	1.486	**0.898**	1.205	1.531	**0.051**	1.209	1.544
20 ≤ VIX < 25	**3.730**	1.017	0.959	**3.064**	1.084	1.000	**0.111**	1.049	0.970
25 ≤ VIX < 30	**5.778**	0.549	0.465	**4.877**	0.532	0.431	**0.165**	0.521	0.424
30 ≤ VIX < 35	**7.220**	0.422	0.489	**6.481**	0.365	0.401	**0.209**	0.357	0.404
35 ≤ VIX	**9.242**	0.512	0.890	**8.061**	0.384	0.822	**0.239**	0.354	0.826
Partitioned by days to maturity									
DTM < 30	**6.486**	0.665	0.933	**4.554**	0.537	0.727	**0.135**	0.506	0.691
30 ≤ DTM < 90	**5.690**	0.734	0.883	**4.102**	0.746	0.852	**0.127**	0.757	0.853
90 ≤ DTM < 150	**6.756**	0.467	0.690	**5.390**	0.461	0.631	**0.177**	0.480	0.660
150 ≤ DTM < 210	**7.095**	0.291	0.579	**5.883**	0.296	0.489	**0.205**	0.343	0.536
210 ≤ DTM	**4.678**	0.336	0.698	**3.132**	0.398	0.711	**0.124**	0.458	0.769

Note: This table reports the out-of-sample VIX futures pricing performance of the three models described in Section 2. We suppress the notations "HAR" for convenience. We use futures contracts for the period starting March 31, 2004 to December 31, 2019 to estimate the parameters and then use VIX futures contracts in 2020 to calculate the pricing errors. The pricing performance is evaluated through the root-mean squared error (RMSE), the mean absolute error (MAE), and the mean absolute percentage error (MAPE). The RMSEs, MAEs, and MAPEs of the benchmark HNG model are in bold font. For the RSV and RV models, we report the ratios of their RMSEs, MAEs, and MAPEs to those of the HNG model. We report the pricing errors for contracts sorted by VIX level and days to maturity.

TABLE 8 | In-sample VIX option pricing performance (Wednesday, 2006–2020).

	RMSE	Ratio to HNG		MAE	Ratio to HNG		MAPE	Ratio to HNG	
	HNG	RSV	RV	HNG	RSV	RV	HNG	RSV	RV
Full sample	**0.816**	0.821	0.913	**0.551**	0.782	0.848	**0.554**	0.688	0.719
Partitioned by moneyness, $m = \log(F/K)$									
$m < -0.4$	**0.494**	0.629	0.639	**0.337**	0.623	0.618	**0.874**	0.601	0.630
$-0.4 \le m < -0.2$	**0.713**	0.730	0.755	**0.517**	0.697	0.724	**0.556**	0.695	0.724
$-0.2 \le m < -0.1$	**0.795**	0.850	0.874	**0.587**	0.831	0.855	**0.396**	0.862	0.842
$-0.1 \le m < 0$	**0.830**	0.918	0.981	**0.629**	0.909	0.967	**0.316**	0.954	0.947
$0 \le m < 0.1$	**0.874**	0.974	1.106	**0.666**	0.969	1.093	**0.244**	1.006	1.067
$0.1 \le m$	**1.348**	0.839	0.984	**0.971**	0.839	0.988	**0.200**	0.884	1.017
Partitioned by days to maturity									
DTM < 20	**0.531**	0.869	0.826	**0.365**	0.799	0.770	**0.587**	0.785	0.701
20 ≤ DTM < 40	**0.611**	0.938	0.957	**0.380**	0.958	0.936	**0.432**	1.000	0.889
40 ≤ DTM < 60	**0.781**	0.889	0.976	**0.479**	0.885	0.963	**0.419**	0.889	0.958
60 ≤ DTM < 80	**0.888**	0.807	0.924	**0.612**	0.759	0.863	**0.575**	0.634	0.735
80 ≤ DTM < 100	**0.957**	0.780	0.898	**0.703**	0.708	0.803	**0.640**	0.518	0.606
100 ≤ DTM	**0.989**	0.760	0.881	**0.750**	0.708	0.791	**0.676**	0.493	0.560

Note: This table reports the in-sample VIX option pricing performance of the three models described in Section 2. We suppress the notations "HAR" for convenience. We use Wednesday call contracts for the period starting on March 1, 2006, and ending on October 15, 2020. The pricing performance is evaluated through the root-mean squared error (RMSE), the mean absolute error (MAE), and the mean absolute percentage error (MAPE). The RMSEs, MAEs, and MAPEs of the benchmark HNG model are in bold font. For the RSV and RV models, we report the ratios of their RMSEs, MAEs, and MAPEs to the HNG model. We report the pricing errors for contracts sorted by moneyness and days to maturity.
Abbreviations: DTM, days to maturity; RSV, realized semivariance; RV, realized variance.

TABLE 9 | Out-of-sample VIX option pricing performance (Thursday, 2006–2020).

	RMSE	Ratio to HNG		MAE	Ratio to HNG		MAPE	Ratio to HNG	
	HNG	RSV	RV	HNG	RSV	RV	HNG	RSV	RV
Full sample	**0.807**	0.831	0.917	**0.547**	0.786	0.852	**0.550**	0.690	0.724
Partitioned by moneyness, $m = \log(F/K)$									
$m < -0.4$	**0.490**	0.668	0.669	**0.339**	0.644	0.640	**0.860**	0.605	0.638
$-0.4 \le m < -0.2$	**0.706**	0.739	0.774	**0.513**	0.697	0.731	**0.553**	0.688	0.725
$-0.2 \le m < -0.1$	**0.806**	0.863	0.891	**0.597**	0.826	0.855	**0.402**	0.857	0.838
$-0.1 \le m < 0$	**0.865**	0.919	0.995	**0.650**	0.910	0.971	**0.322**	0.955	0.943
$0 \le m < 0.1$	**0.923**	0.964	1.087	**0.688**	0.961	1.080	**0.252**	1.004	1.060
$0.1 \le m$	**1.293**	0.845	0.977	**0.924**	0.841	0.988	**0.195**	0.887	1.020
Partitioned by days to maturity									
DTM < 20	**0.562**	0.876	0.839	**0.375**	0.790	0.772	**0.607**	0.763	0.709
20 ≤ DTM < 40	**0.598**	0.919	0.958	**0.382**	0.932	0.940	**0.418**	0.989	0.906
40 ≤ DTM < 60	**0.836**	0.902	0.977	**0.513**	0.886	0.962	**0.434**	0.852	0.943
60 ≤ DTM < 80	**0.851**	0.820	0.927	**0.596**	0.765	0.866	**0.545**	0.641	0.742
80 ≤ DTM < 100	**0.955**	0.794	0.909	**0.700**	0.717	0.813	**0.635**	0.529	0.615
100 ≤ DTM	**0.992**	0.772	0.886	**0.753**	0.713	0.795	**0.686**	0.493	0.566

Note: This table reports the out-of-sample VIX option pricing performance of the three models described in Section 2. We suppress the notations "HAR" for convenience. We use Thursday call contracts for the period starting on March 1, 2006, and ending on October 15, 2020. The pricing performance is evaluated through the root-mean squared error (RMSE), the mean absolute error (MAE), and the mean absolute percentage error (MAPE). The RMSEs, MAEs, and MAPEs of the benchmark HNG model are in bold font. For the RSV and RV models, we report the ratios of their RMSEs, MAEs, and MAPEs to the HNG model. We report the pricing errors for contracts sorted by moneyness and days to maturity.

Abbreviations: DTM, days to maturity; HNG, Heston-Nandi GARCH; RSV, realized semivariance; RV, realized variance.

When examining subgroups categorized by moneyness and days to maturity, the HAR-RSV model's superiority over the HAR-HNG model is particularly evident for deep out-of-the-money and long-term options. In contrast, the HAR-RV model excels in pricing very short-term options.

We further conduct an out-of-sample analysis to evaluate the pricing performance of the HAR-RSV model. We use the parameters estimated using Wednesday VIX option contracts from March 1, 2006 to October 15, 2020 to calculate the errors in pricing Thursday option contracts over the same period. A similar method was also adopted Christoffersen, Jacobs, and Mimouni (2010) and Tong and Huang (2021). Table 9 presents the values of out-of-sample RMSEs, MAEs, and MAPEs of the benchmark HAR-HNG model, as well as the ratios of HAR-RSV's and HAR-RV's pricing errors to the benchmark.

The results shown in Table 9 are very similar to the ones reported in Table 8. The proposed HAR-RSV model still performs best in terms of RMSE, MAE and MAPE, although their outperformance is slightly less pronounced compared with the in-sample case. In the subgroups, the superior pricing performance of the HAR-RSV and HAR-RV models is also similar to that of the in-sample case.

6 | Conclusion

This article employs a realized semivariance-based model to directly depict the dynamics of VIX and studies VIX futures and option pricing under the proposed model. We construct the upside and downside realized semivariance using 5-min VIX data and derive closed-form solutions of VIX futures and option price. The empirical results show that the realized semivariance-based HAR-RSV model generally has the best in- and out-of-sample pricing performance compared with the two competing models, the conventional unsigned realized variance-based HAR-RV model, and the classic HAR-Heston-Nandi GARCH model. The outperformance of the HAR-RSV model is more pronounced for deep out-of-money and longer-term options. The results indicate that the decomposition of realized variance into upside and downside components helps to improve the performance on pricing VIX futures and options.

Acknowledgments

We are grateful for many valuable comments made by participants at the 12th International Conference on Futures and Other Derivatives (ICFOD2023), and the 6th China Derivatives Youth Forum. Zhuo Huang acknowledges financial support from the Fund of the National Natural Science Foundation of China (72271010, 72241418). Chen Tong acknowledges financial support from the Youth Fund of the National Natural Science Foundation of China (72301227) and the Ministry of Education of China, Humanities and Social Sciences Youth Fund (22YJC790117). This research obtained database services from the School of Economics at Xiamen University.

Conflicts of Interest

The authors declare no conflicts of interest.

Data Availability Statement

The high-frequency VIX data can be downloaded from TickData.com, while VIX and VIX futures prices are sourced from the official websites of CBOE (https://www.cboe.com). Additionally, VIX options data are retrieved from OptionMetrics of WRDS. Any other data supporting the findings of this study are available from the corresponding author upon reasonable request.

Endnotes

[1]Other studies on pricing CBOE VIX with discrete-time GARCH models include Hao and Zhang (2013) and Hansen et al. (2024).

[2]The leverage effect refers to the generally negative correlation between an asset return and its changes of volatility (Ait-Sahalia, Fan, and Li 2013).

[3]We test the significance of differences in standard deviations, skewness, and kurtosis using bootstrap method, all three tests reject the null hypothesis of equality, yielding t-statistics of 174.4528 ($p < 0.01$), 146.1762 ($p < 0.01$), and 156.0280 ($p < 0.01$), respectively.

[4]For the HAR-RSV model, the significance tests for β_d, β_w, and β_m resulted in t-statistics of 237.8178, 11.9952, and 100.5920, respectively, all with p-values < 0.01. This indicates that the estimates of β_d, β_w, and β_m are all significantly different from zero, even though the value of β_w is close to zero. Similarly, in the other two models, these three parameters are also significantly different from zero.

References

Ait-Sahalia, Y., J. Fan, and Y. Li. 2013. "The Leverage Effect Puzzle: Disentangling Sources of Bias at High Frequency." *Journal of Financial Economics* 109, no. 1: 224–249.

Barndorff-Nielsen, O. E., S. Kinnebrouk, and N. Shephard. 2010. "Measuring Downside Risk: Realised Semivariance." In *Volatility and Time Series Econometrics: Essays in Honor of Robert F. Engle*, edited by T. Bollerslev, J. Russell, and M. Watson, 117–136. Oxford, England: Oxford University Press.

Cao, H., A. Badescu, Z. Cui, and S. K. Jayaraman. 2020. "Valuation of VIX and Target Volatility Options with Affine GARCH Models." *Journal of Futures Markets* 40, no. 12: 1880–1917.

Christoffersen, P., B. Feunou, K. Jacobs, and N. Meddahi. 2014. "The Economic Value of Realized Volatility: Using High-Frequency Returns for Option Valuation." *Journal of Financial and Quantitative Analysis* 49, no. 3: 663–697.

Christoffersen, P., and K. Jacobs. 2004. "Which GARCH Model for Option Valuation?" *Management Science* 50, no. 9: 1204–1221.

Christoffersen, P., K. Jacobs, and K. Mimouni. 2010. "Volatility Dynamics for the s&p500: Evidence From Realized Volatility, Daily Returns, and Option Prices." *Review of Financial Studies* 23, no. 8: 3141–3189.

Feunou, B., and C. Okou. 2019. "Good Volatility, Bad Volatility, and Option Pricing." *Journal of Financial and Quantitative Analysis* 54, no. 2: 695–727.

Goard, J., and M. Mazur. 2013. "Stochastic Volatility Models and the Pricing of VIX Options." *Mathematical Finance* 23, no. 3: 439–458.

Grünbichler, A., and F. A. Longstaff. 1996. "Valuing Futures and Options on Volatility." *Journal of Banking & Finance* 20, no. 6: 985–1001.

Hansen, P. R., Z. Huang, C. Tong, and T. Wang. 2024. "Realized GARCH, CBOE VIX, and the Volatility Risk Premium." *Journal of Financial Econometrics* 22, no. 1: 187–223.

Hao, J., and J. E. Zhang. 2013. "GARCH Option Pricing Models, the CBOE VIX, and Variance Risk Premium." *Journal of Financial Econometrics* 11, no. 3: 556–580.

Heston, S. L., and S. Nandi. 2000. "A Closed-Form GARCH Option Valuation Model." *The Review of Financial Studies* 13, no. 3: 585–625.

Huang, Z., C. Tong, and T. Wang. 2019. "VIX Term Structure and VIX Futures Pricing with Realized Volatility." *Journal of Futures Markets* 39, no. 1: 72–93.

Jiang, G., G. Qiao, F. Ma, and L. Wang. 2022. "Directly Pricing VIX Futures With Observable Dynamic Jumps Based on High-Frequency VIX." *Journal of Futures Markets* 42, no. 8: 1518–1548.

Jing, B., S. Li, and Y. Ma. 2020. "Pricing VIX Options with Volatility Clustering." *Journal of Futures Markets* 40, no. 6: 928–944.

Lian, G.-H., and S.-P. Zhu. 2013. "Pricing VIX Options with Stochastic Volatility and Random Jumps." *Decisions in Economics and Finance* 36: 71–88.

Lin, Y.-N. 2007. "Pricing VIX Futures: Evidence from Integrated Physical and Risk-Neutral Probability Measures." *Journal of Futures Markets: Futures, Options, and Other Derivative Products* 27, no. 12: 1175–1217.

Lin, Y.-N., and C.-H. Chang. 2009. "VIX Option Pricing." *Journal of Futures Markets: Futures, Options, and Other Derivative Products* 29, no. 6: 523–543.

Luo, X., J. E. Zhang, and W. Zhang. 2019. "Instantaneous Squared VIX and VIX Derivatives." *Journal of Futures Markets* 39, no. 10: 1193–1213.

Mencia, J., and E. Sentana. 2013. "Valuation of VIX Derivatives." *Journal of Financial Economics* 108, no. 2: 367–391.

Park, Y.-H. 2016. "The Effects of Asymmetric Volatility and Jumps on the Pricing of VIX Derivatives." *Journal of Econometrics* 192, no. 1: 313–328.

Patton, A. J., and K. Sheppard. 2015. "Good Volatility, Bad Volatility: Signed Jumps and the Persistence of Volatility." *Review of Economics and Statistics* 97, no. 3: 683–697.

Qiao, G., and G. Jiang. 2023. "VIX Futures Pricing Based on High-Frequency VIX: A Hybrid Approach Combining SVR With Parametric Models." *Journal of Futures Markets* 43, no. 9: 1238–1260.

Sepp, A. 2008. "VIX Option Pricing in a Jump-Diffusion Model." *Risk Magazine*: 84–89.

Song, Z., and D. Xiu. 2016. "A Tale of Two Option Markets: Pricing Kernels and Volatility Risk." *Journal of Econometrics* 190, no. 1: 176–196.

Tong, C. 2024. "Pricing CBOE VIX in Non-Affine GARCH Models With Variance Risk Premium." *Finance Research Letters* 62: 105115.

Tong, C., P. R. Hansen, and Z. Huang. 2022. "Option Pricing With State-Dependent Pricing Kernel." *Journal of Futures Markets* 42, no. 8: 1409–1433.

Tong, C., and Z. Huang. 2021. "Pricing VIX Options With Realized Volatility." *Journal of Futures Markets* 41, no. 8: 1180–1200.

Tong, C., and Z. Huang. 2023. "Good Volatility, Bad Volatility, and VIX Futures Pricing: Evidence From the Decomposition of VIX." *The Journal of Derivatives* 30, no. 3: 117–143.

Tong, C., Z. Huang, and T. Wang. 2022. "Do VIX Futures Contribute to the Valuation of VIX Options?" *Journal of Futures Markets* 42, no. 9: 1644–1664.

Wang, Q., and Z. Wang. 2020. "VIX Valuation and Its Futures Pricing Through a Generalized Affine Realized Volatility Model with Hidden Components and Jump." *Journal of Banking & Finance* 116: 105845.

Wang, T., S. Cheng, F. Yin, and M. Yu. 2022. "Directly Pricing VIX Futures: The Role of Dynamic Volatility and Jump Intensity." *Applied Economics* 54, no. 32: 3678–3694.

Wang, T., Y. Shen, Y. Jiang, and Z. Huang. 2017. "Pricing the CBOE VIX Futures With the Heston-Nandi GARCH Model." *Journal of Futures Markets* 37, no. 7: 641–659.

Yin, F., Y. Bian, and T. Wang. 2021. "A Short Cut: Directly Pricing VIX Futures With Discrete-Time Long Memory Model and Asymmetric Jumps." *Journal of Futures Markets* 41, no. 4: 458–477.

Zhang, J. E., and Y. Zhu. 2006. "VIX Futures." *Journal of Futures Markets: Futures, Options, and Other Derivative Products* 26, no. 6: 521–531.

CBOE VIX Index. 2024. [dataset]. https://www.cboe.com/tradable_products/vix/vix_historical_data/.

CBOE VIX Futures. 2024. [dataset]. https://www.cboe.com/us/futures/market_statistics/historical_data/.

CBOE VIX Options. 2024. [dataset]. Option Metrics of Wharton Research Data Services (WRDS). https://wrds-www.wharton.upenn.edu.

High-frequency VIX Data. 2023. [dataset]. https://www.tickdata.com.

Appendix A

Moment Generating Function Under the HAR-RSV Model

Let $f_{t,T}(\phi)$ be the conditional moment generating function (MGF) of y_T, i.e.,

$$f_{t,T}(\phi) = E_t[\exp(\phi y_T)].$$

Assume that $f_{t,T}(\phi)$ takes the following log-linear form:

$$f_{t,T}(\phi) = \exp\left(A(m,\phi) + \sum_{i=1}^{22} B_i(m,\phi) y_{t+1-i} + C(m,\phi)h_{u,t} + D(m,\phi)h_{d,t}\right), \tag{A1}$$

where $m = T - t$. Applying the law of iterated expectations to $f_{t,T}(\phi)$, we get

$$\begin{aligned} f_{t,T}(\phi) &= E_t[f_{t+1,T}(\phi)] \\ &= E_t\left[\exp\left(A(m-1,\phi) + \sum_{i=1}^{22} B_i(m-1,\phi) y_{t+2-i} \right.\right. \\ &\quad \left.\left. + C(m-1,\phi)h_{u,t+1} + D(m-1,\phi)h_{d,t+1}\right)\right]. \end{aligned}$$

Substituting the dynamics of y_{t+1}, $h_{u,t+1}$ and $h_{d,t+1}$ shows

$$\begin{aligned} f_{t,T}(\phi) = E_t\Bigg[\exp\Bigg(&A(m-1,\phi) + B_1(m-1,\phi)\left(w + \beta_d y_t^{(d)} + \beta_w y_t^{(w)} + \beta_m y_t^{(m)} + \left(\lambda_u - \frac{1}{2}\right)h_{u,t}\right. \\ &\left. + \left(\lambda_d - \frac{1}{2}\right)h_{d,t} + \sqrt{h_{u,t}}\epsilon_{u,t+1}^{(1)} + \sqrt{h_{d,t}}\epsilon_{d,t+1}^{(1)}\right) + \sum_{i=2}^{22} B_i(m-1,\phi) y_{t+2-i} \\ &+ C(m-1,\phi)\left(w_u + b_u h_{u,t} + a_u\left(h_{u,t} + \sigma_u\left[\left(\epsilon_{u,t+1}^{(2)} - \gamma_u\sqrt{h_{u,t}}\right)^2 - \left(1 + \gamma_u^2 h_{u,t}\right)\right]\right)\right) \\ &+ D(m-1,\phi)\left(w_d + b_d h_{d,t} + a_d\left(h_{d,t} + \sigma_d\left[\left(\epsilon_{d,t+1}^{(2)} - \gamma_d\sqrt{h_{d,t}}\right)^2 - \left(1 + \gamma_d^2 h_{d,t}\right)\right]\right)\right)\Bigg)\Bigg]. \end{aligned}$$

Rearranging the terms

$$\begin{aligned} f_{t,T}(\phi) = \exp\Big[&A(m-1,\phi) + B_1(m-1,\phi)w + C(m-1,\phi)w_u - C(m-1,\phi)a_u\sigma_u + D(m-1,\phi)w_d \\ &- D(m-1,\phi)a_d\sigma_d + \left(B_1(m-1,\phi)\left(\lambda_u - \frac{1}{2}\right) + C(m-1,\phi)b_u + C(m-1,\phi)a_u\right)h_{u,t} \\ &+ \left(B_1(m-1,\phi)\left(\lambda_d - \frac{1}{2}\right) + D(m-1,\phi)b_d + D(m-1,\phi)a_d\right)h_{d,t} \\ &+ B_1(m-1,\phi)\left(\beta_d y_t + \frac{1}{4}\beta_w\sum_{i=2}^{5} y_{t+1-i} + \frac{1}{17}\beta_m\sum_{i=6}^{22} y_{t+1-i}\right) + \sum_{i=2}^{22} B_i(m-1,\phi) y_{t+2-i}\Big] \\ &\times E_t\Bigg[\exp\Bigg(B_1(m-1,\phi)\sqrt{h_{u,t}}\epsilon_{u,t+1}^{(1)} + C(m-1,\phi)a_u\sigma_u\left(\left(\epsilon_{u,t+1}^{(2)}\right)^2 - 2\gamma_u\sqrt{h_{u,t}}\epsilon_{u,t+1}^{(2)}\right) \\ &+ B_1(m-1,\phi)\sqrt{h_{d,t}}\epsilon_{d,t+1}^{(1)} + D(m-1,\phi)a_d\sigma_d\left(\left(\epsilon_{d,t+1}^{(2)}\right)^2 - 2\gamma_d\sqrt{h_{d,t}}\epsilon_{d,t+1}^{(2)}\right)\Bigg)\Bigg]. \end{aligned} \tag{A2}$$

A useful result is that for a standard normal random variable ϵ,

$$E[\exp(a\epsilon + b\epsilon^2)] = \frac{1}{\sqrt{1-2b}}\exp\left(\frac{a^2/2}{1-2b}\right).$$

Substituting this result in Equation (A2) and matching the terms on the right-hand side of Equations (A1) and (A2), we can get the following recursive formulae,

$$
\begin{aligned}
A(m+1,\phi) &= A(m,\phi) + B_1(m,\phi)w + C(m,\phi)w_u - C(m,\phi)a_u\sigma_u + D(m,\phi)w_d \\
&\quad - D(m,\phi)a_d\sigma_d - \frac{1}{2}\ln(1-2C(m,\phi)a_u\sigma_u) - \frac{1}{2}\ln(1-2D(m,\phi)a_d\sigma_d), \\
C(m+1,\phi) &= B_1(m,\phi)\left(\lambda_u - \frac{1}{2}\right) + C(m,\phi)b_u + C(m,\phi)a_u + \frac{1}{2}\frac{B_1^2(m,\phi)}{1-2C(m,\phi)a_u\sigma_u} \\
&\quad + \frac{C(m,\phi)a_u\sigma_u\left(2\gamma_u^2 C(m,\phi)a_u\sigma_u - 2\gamma_u B_1(m,\phi)\rho_u - B_1^2(m,\phi)\left(1-\rho_u^2\right)\right)}{1-2C(m,\phi)a_u\sigma_u}, \\
D(m+1,\phi) &= B_1(m,\phi)\left(\lambda_d - \frac{1}{2}\right) + D(m,\phi)b_d + D(m,\phi)a_d + \frac{1}{2}\frac{B_1^2(m,\phi)}{1-2D(m,\phi)a_d\sigma_d} \\
&\quad + \frac{D(m,\phi)a_d\sigma_d\left(2\gamma_d^2 D(m,\phi)a_d\sigma_d - 2\gamma_d B_1(m,\phi)\rho_d - B_1^2(m,\phi)\left(1-\rho_d^2\right)\right)}{1-2D(m,\phi)a_d\sigma_d},
\end{aligned}
$$

$$
B_i(m+1,\phi) = \begin{cases} B_1(m,\phi)\beta_d + B_2(m,\phi) & i = 1, \\ \frac{1}{4}B_1(m,\phi)\beta_w + B_{i+1}(m,\phi) & 2 \le i \le 5, \\ \frac{1}{17}B_1(m,\phi)\beta_m + B_{i+1}(m,\phi) & 6 \le i \le 21, \\ \frac{1}{17}B_1(m,\phi)\beta_m & i = 22. \end{cases}
$$

The terminal condition is $B_1(0,\phi) = \phi$, $B_i(0,\phi) = 0$ for $i \ge 2$, $A(0,\phi) = C(0,\phi) = D(0,\phi) = 0$.

Appendix B

Moment Generating Function Under the HAR-RV Model

Let $f_{t,T}(\phi)$ be the conditional moment generating function (MGF) of y_T, that is,

$$
f_{t,T}(\phi) = E_t[\exp(\phi y_T)].
$$

Assume the MGF takes the following log-linear form:

$$
f_{t,T}(\phi) = \exp\left(A(m,\phi) + \sum_{i=1}^{22} B_i(m,\phi)y_{t+1-i} + C(m,\phi)h_t\right), \quad \text{(B1)}
$$

where $m = T - t$. Applying the law of iterated expectations to $f_{t,T}(\phi)$, we get

$$
f_{t,T}(\phi) = E_t[f_{t+1,T}(\phi)] = E_t\left[\exp\left(A(m-1,\phi) + \sum_{i=1}^{22} B_i(m-1,\phi)y_{t+2-i} + C(m-1,\phi)h_{t+1}\right)\right].
$$

Substituting the dynamics of y_{t+1} and h_{t+1} shows

$$
\begin{aligned}
f_{t,T}(\phi) = E_t\Bigg[\exp\Bigg(&A(m-1,\phi) + B_1(m-1,\phi)\Bigg(w + \beta_d y_t^{(d)} \\
&+ \beta_w y_t^{(w)} + \beta_m y_t^{(m)} + \left(\lambda - \frac{1}{2}\right)h_t + \sqrt{h_t}\epsilon_{t+1}^{(1)}\Bigg) \\
&+ \sum_{i=2}^{22} B_i(m-1,\phi)y_{t+2-i} + C(m-1,\phi) \\
&\left(w_h + bh_t + a\left(h_t + \sigma\left[\left(\epsilon_{t+1}^{(2)} - \gamma\sqrt{h_t}\right)^2 - \left(1+\gamma^2 h_t\right)\right]\right)\right)\Bigg)\Bigg].
\end{aligned}
$$

Rearranging the terms

$$
\begin{aligned}
f_{t,T}(\phi) = \exp\Big[&A(m-1,\phi) + B_1(m-1,\phi)w + C(m-1,\phi)w_h - C(m-1,\phi)a\sigma \\
&+ \left(B_1(m-1,\phi)\left(\lambda - \frac{1}{2}\right) + C(m-1,\phi)(b+a)\right)h_t \\
&+ B_1(m-1,\phi)\left(\beta_d y_t + \frac{1}{4}\beta_w\sum_{i=2}^{5} y_{t+1-i} + \frac{1}{17}\beta_m\sum_{i=6}^{22} y_{t+1-i}\right) + \sum_{i=2}^{22} B_i(m-1,\phi)y_{t+2-i}\Big] \\
&\times E_t\left[\exp\left(B_1(m-1,\phi)\sqrt{h_t}\epsilon_{t+1}^{(1)} + C(m-1,\phi)a\sigma\left(\left(\epsilon_{t+1}^{(2)}\right)^2 - 2\gamma\sqrt{h_t}\epsilon_{t+1}^{(2)}\right)\right)\right].
\end{aligned} \quad \text{(B2)}
$$

A useful result is that for a standard normal random variable ϵ,

$$E[\exp(a\epsilon + b\epsilon^2)] = \frac{1}{\sqrt{1-2b}}\exp\left(\frac{a^2/2}{1-2b}\right).$$

Substituting this result in Equation (B2) and matching the terms on the right-hand side of Equations (B1) and (B2), we can get the following recursive formulae,

$$\begin{aligned}
A(m+1,\phi) &= A(m,\phi) + B_1(m,\phi)w + C(m,\phi)(w_h - a\sigma) - \frac{1}{2}\ln(1-2C(m,\phi)a\sigma),\\
C(m+1,\phi) &= B_1(m,\phi)\left(\lambda - \frac{1}{2}\right) + C(m,\phi)(b+a) + \frac{1}{2}\frac{B_1^2(m,\phi)}{1-2C(m,\phi)a\sigma}\\
&\quad + \frac{C(m,\phi)a\sigma\left(2\gamma^2 C(m,\phi)a\sigma - 2\gamma B_1(m,\phi)\rho - B_1^2(m,\phi)(1-\rho^2)\right)}{1-2C(m,\phi)a\sigma},
\end{aligned}$$

$$B_i(m+1,\phi) = \begin{cases} B_1(m,\phi)\beta_d + B_2(m,\phi) & i = 1,\\ \frac{1}{4}B_1(m,\phi)\beta_w + B_{i+1}(m,\phi) & 2 \le i \le 5,\\ \frac{1}{17}B_1(m,\phi)\beta_m + B_{i+1}(m,\phi) & 6 \le i \le 21,\\ \frac{1}{17}B_1(m,\phi)\beta_m & i = 22. \end{cases}$$

The terminal condition is $B_1(0,\phi) = \phi$, $B_i(0,\phi) = 0$ for $i \ge 2$, $A(0,\phi) = C(0,\phi) = 0$.

where $m = T - t$. Applying the law of iterated expectations to $f_{t,T}(\phi)$, we get

$$f_{t,T}(\phi) = E_t[f_{t+1,T}(\phi)] = E_t\left[\exp\left(A(m-1,\phi) + \sum_{i=1}^{22} B_i(m-1,\phi)y_{t+2-i} + C(m-1,\phi)h_{t+1}\right)\right].$$

Substituting the dynamics of y_{t+1} and h_{t+1} shows

$$\begin{aligned}
f_{t,T}(\phi) = E_t\Bigg[\exp\Bigg(&A(m-1,\phi) + B_1(m-1,\phi)\Bigg(w + \beta_d y_t^{(d)} + \beta_w y_t^{(w)}\\
&+ \beta_m y_t^{(m)} + \left(\lambda - \frac{1}{2}\right)h_t + \sqrt{h_t}\epsilon_{t+1}\Bigg)\\
&+ \sum_{i=2}^{22} B_i(m-1,\phi)y_{t+2-i} + C(m-1,\phi)(w_h + bh_t\\
&+ a(\epsilon_{t+1} - \gamma\sqrt{h_t})^2)\Bigg)\Bigg].
\end{aligned}$$

Rearranging the terms

$$\begin{aligned}
f_{t,T}(\phi) = \exp\Big[&A(m-1,\phi) + B_1(m-1,\phi)w + C(t+1;T,\phi)w_h\\
&+ \left(B_1(m-1,\phi)\left(\lambda - \frac{1}{2}\right) + C(m-1,\phi)(b+a\gamma)\right)h_t\\
&+ B_1(m-1,\phi)\left(\beta_d y_t + \frac{1}{4}\beta_w\sum_{i=2}^{5} y_{t+1-i} + \frac{1}{17}\beta_m\sum_{i=6}^{22} y_{t+1-i}\right) + \sum_{i=2}^{22} B_i(m-1,\phi)y_{t+2-i}\Big]\\
&\times E_t\left[\exp\left(B_1(m-1,\phi)\sqrt{h_t}\epsilon_{t+1} + C(m-1,\phi)a\left(\epsilon_{t+1}^2 - 2\gamma\sqrt{h_t}\epsilon_{t+1}\right)\right)\right].
\end{aligned} \tag{C2}$$

Appendix C

Moment Generating Function Under the HAR-HNG Model

Let $f_{t,T}(\phi)$ be the conditional moment generating function (MGF) of y_T, that is,

$$f_{t,T}(\phi) = E_t[\exp(\phi y_T)].$$

Assume the MGF takes the following log-linear form:

$$f_{t,T}(\phi) = \exp\left(A(m,\phi) + \sum_{i=1}^{22} B_i(m,\phi)y_{t+1-i} + C(m,\phi)h_t\right), \tag{C1}$$

A useful result is that for a standard normal random variable ϵ,

$$E[\exp(a\epsilon + b\epsilon^2)] = \frac{1}{\sqrt{1-2b}}\exp\left(\frac{a^2/2}{1-2b}\right).$$

Substituting this result in Equation (C2) and matching the terms on the right-hand side of Equations (C1) and (C2), we can get the following recursive formulae,

$$A(m+1,\phi) = A(m,\phi) + B_1(m,\phi)w + C(m,\phi)w_h - \frac{1}{2}\ln(1-2C(m,\phi)a),$$
$$C(m+1,\phi) = B_1(m,\phi)\left(\lambda - \frac{1}{2}\right) + C(m,\phi)(b + a\gamma^2) + \frac{1}{2}\frac{B_1^2(m,\phi) + 4C^2(m,\phi)a^2\gamma^2 - 4B_1(m,\phi)C(m,\phi)a\gamma}{1-2C(m,\phi)a},$$

with

$$B_i(m+1,\phi) = \begin{cases} B_1(m,\phi)\beta_d + B_2(m,\phi) & i = 1, \\ \frac{1}{4}B_1(m,\phi)\beta_w + B_{i+1}(m,\phi) & 2 \le i \le 5, \\ \frac{1}{17}B_1(m,\phi)\beta_m + B_{i+1}(m,\phi) & 6 \le i \le 21, \\ \frac{1}{17}B_1(m,\phi)\beta_m & i = 22. \end{cases}$$

The terminal condition is $B_1(0,\phi) = \phi$, $B_i(0,\phi) = 0$ for $i \ge 2$, $A(0,\phi) = C(0,\phi) = 0$.